Computers and Chemical Engineering 34 (2010) 1049–1057

Contents lists available at ScienceDirect

Computers and Chemical Engineering

journal homepage: www.elsevier.com/locate/compchemeng

Practical application of roller compaction process modeling

Gavin Reynolds [a], Rohit Ingale [b,*], Ron Roberts [a], Sanjeev Kothari [b], Bindhu Gururajan [c]

[a] Pharmaceutical and Analytical Research and Development, AstraZeneca, Silk Road Business Park Charter Way, Macclesfield, Cheshire SK10 2NA, UK
[b] Pharmaceutical and Analytical Research and Development, AstraZeneca, Concord Pike, Wilmington, DE 19850, USA
[c] Pharmaceutical and Analytical Research and Development, AstraZeneca, Charnwood Bakewell Road, Loughborough, Leicestershire LE11 5RH, UK

ARTICLE INFO

Article history:
Received 31 August 2009
Received in revised form 5 March 2010
Accepted 9 March 2010
Available online 16 March 2010

Keywords:
Roller compaction
Dry granulation
Pharmaceutical
Modeling
Ribbon density
Scale-up

ABSTRACT

Very limited work has been reported on comparing the performance of the roller compaction process at different scales. The majority of the approaches highlighted in the literature discuss the applicability of using confined uniaxial compaction for predicting the performance of the roller compaction process. In this paper a method was developed that allows the rolling theory of granular solids developed by Johanson [Johanson, J. R. (1965). A rolling theory for granular solids. *ASME, Journal of Applied Mechanics Series E*, *32*(4), 842–848] to be used to infer the underlying material parameters from small-scale roller compaction experiments for both separation controlled or screw controlled configurations. Once these parameters are determined, the model can be used for predictive process design and scale-up in order to achieve target outputs such as ribbon density and throughput. The peak pressure, predicted by the model, can also be used to present roller compaction of a given formulation from a scale-independent perspective. This approach can be used to justify process parameter and equipment flexibility in the context of a pharmaceutical design space based on a proven acceptable range of peak pressures, or achieving target intermediate quality attributes, such as ribbon density.

1. Introduction

Roller compaction is a continuous dry granulation process that involves the densification of dry powders into a solid mass (compact). This densification process is achieved by controlled feeding of powder through a set of directly opposed, counter-rotating rollers with a controllable aperture (roller separation or gap) between the rollers. The feed powder is passed through two counter-rotating rolls with the flow being induced by the friction acting at the surfaces of the rolls. In the narrow region of the gap between the rolls, the powder is subjected to high pressure, leading to the formation of a compact or briquette that is reduced in size by milling or screening to achieve the desired granule size. Roller compaction is designed to increase the bulk density and uniformity of particulate formulations, for example, to prevent the segregation of pharmaceutical drugs. It offers unique advantages for processing physically or chemically moisture-sensitive materials since the use of a liquid binder is not required. Another advantage is that it does not require a drying stage and therefore it is suitable for compounds that either have a low melting point or degrade rapidly upon heating (Adeyeye, 2000; Guigon, Simon, Saleh, Bindhumadhavan, & Seville, 2006; Miller, 1997; Pietsch, 1991; Seville, Perera, Greenwood, & Bentham, 2001).

Despite being superficially a simple process, a quantitative understanding has proved difficult to develop because of the complex behavior of particulate materials. Sub-optimal design and operation of the equipment can lead to unsatisfactory products. Current industrial roller compacting practice is based on empirical approach which is time consuming and expensive. The widespread use of roller compaction operation has driven the need to utilize mathematical models for roller compaction process modeling to gain better understanding of the process, and to achieve desired process performance.

Over the past few decades, several approaches have been used to model the roller compaction process. Some of the early work was initiated by Johanson (1965) who developed a powder mechanics model that enabled the roll surface pressure, torque and separating force of the rolls to be predicted from the physical characteristics of the powder and the dimensions of the rollers. However very limited work has highlighted the practical application of this approach (Bindhumadhavan, Seville, Adams, Greenwood, & Fitzpatrick, 2005). Katashinskii (1986) developed a slab analysis method to predict the pressure distribution and roll separation force in metal powder rolling processes. Subsequent work by Dec (1991) highlighted the limitations and discrepancies of the slab method. Recent modeling approaches involve the

* Corresponding author. Tel.: +1 3028854059; fax: +1 3028865375.
E-mail address: rohit.ingale@astrazeneca.com (R. Ingale).

0098-1354/$ – see front matter © 2010 Elsevier Ltd. All rights reserved.
doi:10.1016/j.compchemeng.2010.03.004

Nomenclature

c_S	screw constant [kg]
D	roller diameter [m]
F	force factor [–]
ffc	flow function [–]
K	material compressibility [–]
$\dot{m}_R$	Ribbon mass throughput [kg/s]
$\dot{m}_S$	mass throughput conveyed by screw feeder [kg/s]
N_R	roller speed [s^{-1}]
N_S	screw speed [s^{-1}]
P_{max}	peak pressure [Pa]
R_f	roll force [N]
S	roller separation [m]
W	roller width [m]
α	nip angle [°]
γ	relative density [–]
γ_0	preconsolidation relative density [–]
γ_R	ribbon relative density [–]
δ_E	effective angle of internal friction [°]
ρ	ribbon/bulk density [kg/m^3]
ρ_{true}	material true density [kg/m^3]
ϕ_W	angle of wall friction [°]
θ	Angular roll position [°]
σ_θ	Normal stress at $\theta = \theta$ [Pa]
σ	normal stress [Pa]
σ_α	Normal stress at $\theta = \alpha$ [Pa]
$\bar{v}$	average speed [m/s]
μ	friction coefficient [–]
ε	porosity [–]

use of more advanced finite element models (Dec, Zavaliangos, & Cunningham, 2003), which incorporate information pertaining to powder behavior, geometry, and frictional interactions. Other modeling techniques such as that developed by Zinchuk, Mullarney, and Hancock (2004) involve simulating the roller compaction process using a laboratory scale compaction simulator. The proposed method was based on simulating the compression events that occur during roller compaction using a compaction simulator. This method enables prediction of the effects of processing parameters like roll speed, pressure and diameter on the product quality as characterized by ribbon solid fraction and tensile strength. An important advantage of this method is the small amount of material requirement for roller compaction simulation experiments. The simulation and key compact property approach was proposed in this work for process specific predictive and scale-up studies. Loginov, Bourkine, and Babailov (2001) reported the development of a new roll briquetting simulator for understanding the densification and performance of the roll compaction process. They also developed a mathematical model to relate the results obtained with the laboratory scale to industrial scale. Gereg and Cappola (2002) developed a method to determine the suitability of a drug candidate for roll compaction. Optimum process parameters were determined for lab-scale equipment and these values were then used in the industrial scale. A hydraulic press with a flat-faced punch and die was used as the lab-scale equipment. Both methods for densifying lactose resulted in a product with similar density, compactability and suitable powder flow. The density and hardness of the tablets produced using the granules produced by both the methods were comparable indicating a possible method for determining the suitability of powders for roll compaction.

Scale-up of the roller compaction process can be achieved to a limited extent by increasing throughput (by increasing roller speed, roller gap or screw speed) for a given piece of equipment. Further increase in throughput can only be achieved by increasing the geometric dimensions, such as roller width and roller diameter. Very limited work has been reported on comparing the performance of the roller compaction process at two different scales. Majority of the approaches highlighted in the literature discuss the applicability of using uniaxial compaction for predicting the performance of the roller compaction process.

Hence, the objective of this work was to present a practical approach for roller compaction process modeling and scale-up, which makes use of available or existing process data for estimation of model (material and equipment) parameters followed by utilization of the predictive capability of the model to achieve desired process performance. As a first step, the roller compaction process was modeled using a powder mechanics model proposed by Johanson (1965). As described earlier this simplified model takes into account the physical characteristics of the powder and equipment geometry for predicting the behavior of material undergoing roller compaction. Ribbon relative density was used as an indicator of roller compacted product quality. Numerous investigations (Davies & Newton, 1996; Hancock, Colvin, Mullarney, & Zinchuk, 2003; Rowe & Roberts, 1996; Zinchuk et al., 2004) have shown that material relative density is an important product attribute, which is directly linked to mechanical properties of the material. Thus the ribbon relative density is a key intermediate product attribute which is strongly correlated with the granule and tablet properties. The model parameters were determined from available roller compaction experimental data using a developmental formulation. This step was followed by verification of modeling predictions using the estimated model parameters. Once the predictive capability of the model was established, the model was utilized to predict process parameter settings to achieve desired product properties across two scales. The results obtained, demonstrate the validity and practical utility of the proposed roller compaction modeling strategy.

2. Roller compaction modeling

2.1. General model

During roller compaction, powder is fed between two counter-rotating rolls. The material is continuously compacted and deformed into a solid mass, or ribbon. Key to linking process parameters with the densification of material is determination of the pressure distribution between the rolls. Using powder mechanics theory developed by Jenike and Shield (1959), Johanson (1965) developed a rolling theory for granular solids to describe this pressure distribution. The equation of the effective yield locus is combined with the equations of equilibrium, resulting in a hyperbolic system of partial differential equations. These equations can be solved, using the appropriate boundary conditions. An important aspect of this is determination of the 'nip' angle (α), defined as the angle at which the boundary condition between the material and the rolls changes from a slip condition (in the slip region) to a no-slip condition (in the nip region) as shown in Fig. 1.

For these two boundary conditions, a relationship for the pressure distributions for slip and no-slip can be determined.

$$\left.\frac{d\sigma}{dx}\right|_{Slip} = \frac{4\sigma(\pi/2 - \theta - \nu)\tan\delta_E}{D/2(1 + S/D - \cos\theta)(\cot(A - \mu) - \cot(A + \mu))} \quad (1)$$

$$\left.\frac{d\sigma}{dx}\right|_{Nip} = \frac{K\sigma_\theta(2\cos\theta - 1 - S/D)\tan\theta}{D/2(1 + S/D - \cos\theta)\cos\theta} \quad (2)$$

where

$$A = \frac{\theta + \nu + \pi/2}{2} \quad (3)$$

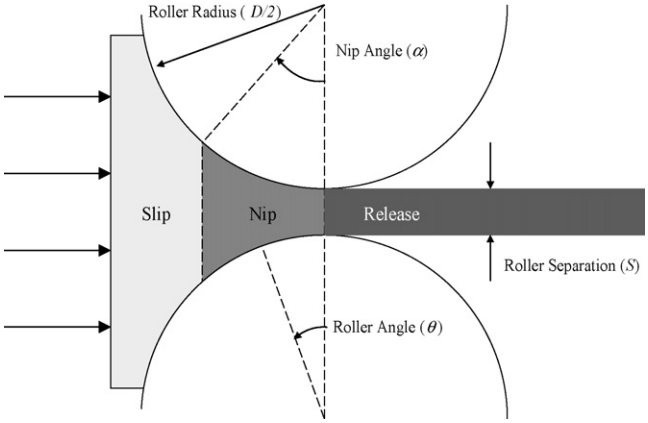

Fig. 1. Schematic diagram of the roller compaction process.

$$2\nu = \pi - \arcsin\left(\frac{\sin\phi_W}{\sin\delta_E}\right) - \phi_W \tag{4}$$

$$\sigma_\theta = \sigma_\alpha\left[\frac{(1+S/D-\cos\alpha)\cos\alpha}{(1+S/D-\cos\theta)\cos\theta}\right]^K \tag{5}$$

Johanson (1965) proposed that the nip angle can be determined by finding the angle at which the pressure gradients for the slip and no-slip conditions were equal. Hence, the nip angle can be determined by equating Eqs. (1) and (2) and solving:

$$\frac{4(\pi/2-\alpha-\nu)\tan\delta_E}{(\cot(A-\mu)-\cot(A+\mu))} = \frac{K(2\cos\alpha-1-S/D)\tan\alpha}{\cos\alpha} \tag{6}$$

Once the nip angle has been determined, the pressure distribution between the rolls can be calculated from Eq. (5). Bindhumadhavan et al. (2005) used an instrumented roll compactor fitted with a miniature piezoelectric transducer in order to measure the pressure profile normal to the roll surface. They found that the pressure distribution is reasonably predicted from Eq. (5), although the measured pressure increased more strongly than the predicted as the material enters the nip region. They also found that the peak pressure applied was very accurately predicted.

The utility of the model is the link between process parameters and material attributes. The pressure is typically applied to the rolls as an overall hydraulic pressure or pressing force (R_f). The relationship for the pressure distribution between the rolls can be used to relate this process parameter with the peak pressure (P_{max}) applied at minimum separation:

$$R_f = \frac{P_{max}WDF}{2} \tag{7}$$

where

$$F = \int_{\theta=0}^{\theta=\alpha(\delta_E,\phi_W,K)}\left[\frac{S/D}{(1+S/D-\cos\theta)\cos\theta}\right]^K\cos\theta\,d\theta \tag{8}$$

This represents a relationship between process parameters (roll force (R_f), roll separation (S)), geometric parameters (roll diameter (D), roll width (W)) and material properties (effective angle of internal friction (δ_E), angle of wall friction (ϕ_W) and compressibility (K)).

The ribbon relative density (defined as 1 minus the pore volume fraction) is a key intermediate attribute for roller compaction processes, which can often be related to downstream product attributes. Eq. (5) is based on a simple power law relationship between material density and pressure. Following this, the relative density of the ribbon (γ_R) can be estimated from the peak pressure as follows:

$$\gamma_R = \gamma_0 P_{max}^{1/K} \tag{9}$$

Here, γ_0 is referred to as the preconsolidation relative density. The relationship between relative density (γ), porosity (ε), bulk density (ρ) and true density (ρ_{true}) is shown below:

$$\gamma = 1-\varepsilon = \frac{\rho}{\rho_{true}} \tag{10}$$

Eqs. (7)–(9) can then be used to concisely relate process parameters, equipment geometry and powder material properties to the output of the roll compactor in terms of ribbon relative density:

$$\gamma_R = \gamma_0\left(\frac{2R_f}{WD\int_{\theta=0}^{\theta=\alpha(\delta_E,\phi_W,K)}[(S/D)/((1+S/D-\cos\theta)\cos\theta)]^K\cos\theta\,d\theta}\right)^{1/K} \tag{11}$$

2.2. Extension of general model to include screw speed

A common configuration in the design of roll compactors is the use of a screw conveyor to transport powder to the nip region. In some instances, the roll separation cannot be controlled directly and the speed of the screw conveyor is the key process parameter. The general model outlined in Section 2.1 includes the roll separation. If this is not known or not controlled directly, then it is useful to be able to use screw speed as a process parameter in the equations.

Fig. 2 shows a schematic diagram of a segment of material passing between the rolls at the minimum separation point. From a mass balance, the mass flow rate of material, $\dot{m}$, can be written as:

$$\dot{m}_R = \rho_{true}\gamma_R\bar{v}WS \tag{12}$$

where $\bar{v}$ is the average speed of the material between the rollers, W is the roller width, S is the roll separation and γ_R is the relative density of the ribbon. Assuming no-slip at the roller surface in this region (i.e. material is moving at the same speed as the rollers):

$$\bar{v} = \pi DN_R \tag{13}$$

where N_R is the rotation rate of the rolls.

For a screw conveyor, the mass flowrate is typically proportional to the screw rotation rate:

$$\dot{m}_S = c_S N_S \tag{14}$$

At steady state, and assuming negligible side-seal leakage, all the material passing through the screw conveyor should pass between the rolls. Therefore, equating Eqs. (12) and (14), and using Eq. (13):

$$\frac{N_S}{N_R} = \frac{\pi}{c_s}\rho_{true}\gamma_R DWS \tag{15}$$

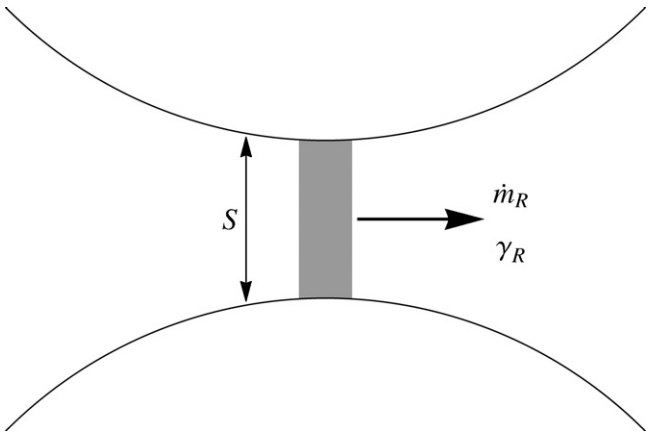

Fig. 2. Schematic diagram of a segment of material passing through a roller compactor.

This equation provides a direct relationship between screw speed, roll speed and roll separation, allowing Eq. (11) to be recast in terms of screw speed, rather than roll separation:

$$\gamma_R = \gamma_0(2R_f)^{1/K}\left(WD\int_{\theta=0}^{\theta=\alpha(\delta_E,\phi_W,K)}\left[\frac{c_S N_S}{\pi\rho_{true}\gamma_R WD^2 N_R(1+c_S N_S/\pi\rho_{true}\gamma_R WD^2 N_R-\cos\theta)\cos\theta}\right]^K\cos\theta\,d\theta\right)^{-1/K} \quad (16)$$

2.3. Estimation of model parameters

In order to solve Eqs. (11) and (16) a number of parameters need to be obtained. These are now discussed in more detail.

2.3.1. Equipment parameters

As already discussed, roll pressure or roll force is typically specified over the entire roll. Roll force (R_f) is sometimes available to specify directly in some equipment. In this case, it can be used directly in Eqs. (11) and (16). On other equipment, roll hydraulic pressure is specified in order to apply a specific force. In this case, a calibration is required between the roll hydraulic pressure and the applied roll force. The calibration can then be used to determine the roll force (R_f) applied for a given set point of roll hydraulic pressure.

For equipment with screw conveyors, the screw constant, c_S (see Eq. (14)) needs to be determined if it is desired or necessary to control the process using screw speed, rather than specifying a roll separation. The screw constant is also useful to determine whether certain combinations of other process parameters are achievable, given the range of available screw speeds. For example, a given combination of roll speed and gap size may require a screw speed below or above its operational range. Knowledge of the screw constant will allow inappropriate combinations of these process parameters to be determined in advance of running the process. The screw constant can be estimated from Eq. (14) or Eq. (15). Using Eq. (14) the mass throughput of the roller compactor can be measured directly by weighing material for a certain period of time, assuming all the material conveyed by the screw passes through the rolls. Alternatively, Eq. (15) can be used provided all process parameters are known (screw speed, roll speed, roll separation) and the ribbon relative density is known. If roll separation is not known, this can be estimated by measuring ribbon thickness. This approach assumes that the elastic recovery of the ribbon is negligible. However, in practice, even some small elastic recovery is likely to fall within the accuracy of determining this parameter.

2.3.2. Material parameters

The key material parameters that are required are flow properties (effective angle of internal friction (δ_E), angle of wall friction (ϕ_W)), compressibility (K), preconsolidation relative density (γ_0), the material true density (ρ_{true}) and the ribbon density (γ_R). The material true density and ribbon density need to be measured using appropriate experimental procedures (as described in Section 3.5). The flow properties are typically measured using a shear cell as described in Section 3.2. Finally, compressibility (and the preconsolidation relative density) values are typically obtained from uniaxial compression as described in Section 3.3.

In practice, there may exist historical or experimental data for a formulation on a particular roller compactor. Data may comprise of process settings, a measure of output quality (ribbon relative density) and throughput.

If sufficient historical or experimental data are available from running a formulation on a roll compactor, then compaction parameters (compressibility and preconsolidation density) can be estimated from the model as follows. From the logarithm of Eq. (9), a linear equation can be obtained:

$$\log(\gamma_R) = \frac{1}{K}\log(P_{max}(K)) + \log(\gamma_0) \quad (17)$$

The peak pressure, P_{max}, can be determined from either Eq. (11) or (16). Note that P_{max} is also a function of the parameters that are to be fitted (K, and γ_0 in the case of Eq. (16)). Eq. (17) can be solved by linear regression in an iterative fashion, converging on the fitted values for compressibility and preconsolidation relative density. If the range of data available for ribbon density is limited, there may be errors from the linear regression approach. If this is the case, the compressibility should be measured (for example from a confined uniaxial compression test), but the preconsolidation density can still be fitted to ensure a good level of prediction for ribbon density. The preference for fitting the preconsolidation density is explored further in the results and discussion (see Section 4.2).

Flow properties are used in the determination of the nip angle (Eq. (6)). Using Eq. (11), the sensitivity of the predicted ribbon relative density as a function of effective angle of internal friction and angle of wall friction can be explored. Fig. 3 shows the output of this analysis using arbitrary geometry and compaction parameters, demonstrating that the predicted ribbon relative density only changes slowly as a function of these flow properties, except for very low values of internal friction and wall friction angles. Taking this into account, the flow properties can be estimated and held constant when fitting the other material parameters (preconsolidation density and/or compressibility).

2.4. Utilization of model for process design

Once calibrated to a particular material, the model is useful for predicting ribbon density as a function of process parameters and equipment geometry. However, in practice it is more useful to be able to specify the outputs of the roll press and then determine the most appropriate process parameters for a given piece of equipment. The typical output will be the key intermediate attribute of ribbon density. Additionally, a certain throughput may be desired to facilitate manufacture scheduling. Fig. 4 shows the influence of process settings (roll force and roll separation) on ribbon relative density and mass throughput (using Eqs. (11) and (12)). If ribbon relative density is the desired output, there exists a range of potential combinations of process settings (roll force and roll separation)

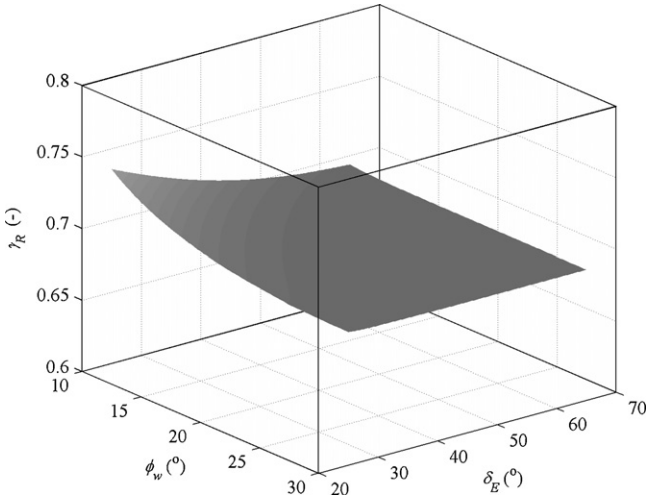

Fig. 3. Analysis showing predicted ribbon relative density (γ_R) as a function of flow properties (effective angle of internal friction, δ_E, and angle of wall friction, ϕ_W). Other parameters were arbitrarily chosen ($\gamma_0 = 0.38$, $K = 8$, $D = 0.1$ m, $W = 0.05$ m).

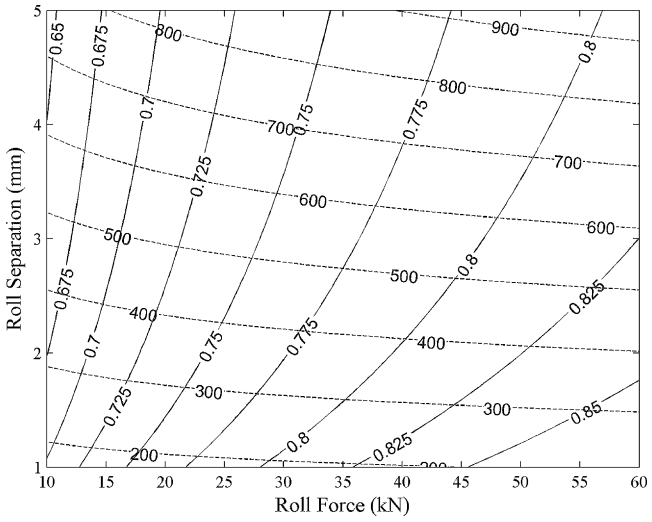

Fig. 4. The influence of process settings (roll force and roll separation) on ribbon relative density (solid contours) and mass throughput in g/min (dashed contours). Mass throughput corresponds to a roll speed of 10 rpm. Plot generated using arbitrary material ($\gamma_0 = 0.4$, $K = 9$, $\delta_E = 40^\circ$, $\phi_W = 20^\circ$), and geometric ($D = 0.1$ m, $W = 0.05$ m) parameters.

that may be selected. Further constraining the output to achieve a target throughput, leads to a smaller subset of combinations that will depend on roll speed. Application of this approach for a change in roller compactor geometry will be explored in the results section (see Section 4.5).

3. Materials and methods

3.1. Formulation

An immediate release development formulation was utilized for this work, which had the following key properties: high drug load (greater than 30%), highly cohesive and adhesive active pharmaceutical ingredient (needle shaped crystals) and poor blend flow properties (Carr's index ~33 and Flow function (*ffc*) ~2.5). The formulation comprised of excipients typically used for immediate release tablets. The major excipients in the formulation were microcrystalline cellulose and dibasic calcium phosphate dihydrate.

3.2. Flow property measurement

A ring shear tester (RST-XS, Dietmar Shultze) was used to measure the flow properties of the formulation blend. The method of operation is based on the principle of rotational shearing. A standard shear testing procedure (Peschl & Colijn, 1977) was used to measure the flow function coefficient (*ffc*), effective angle of internal friction (δ_E), and angle of wall friction (ϕ_W). Flow property measurements were made using preconsolidation loads of 4 kPa and pre-shear stress of 1 kPa, 1.4 kPa, 2 kPa and 2.6 kPa. The effective angle of internal friction, δ_E, and angle of wall friction (against stainless steel coupon with Ra value of 0.4), ϕ_W, were found to be 53° and 20° respectively. The average value of flow function (*ffc*) was found to be 2.5, which can be classified as *cohesive* (Schulze, 1996).

3.3. Compaction properties

The compaction properties (compressibility factor (K) and preconsolidation relative density (γ_0)), can be determined from the actual roller compaction experimental data as described in Section 2.3.2 Alternatively these compaction properties of the formulation blend can be determined using a uniaxial compression die-punch test set up. Powder blend samples of mass 0.5 g were compacted using an Insight 30 (MTS systems Corp., Eden Prairie, MN, USA) compression apparatus and a custom made rectangular die (7 mm × 20 mm) with maximum test pressures ranging from 20 to 200 MPa and at a constant compaction speed of 1 mm/s. The bulk densities of the compacts produced at different compaction pressures were estimated from the punch displacement. The compressibility factor (K) is defined as the reciprocal of the slope of the linear portion of a log density vs. log pressure profile (see Eq. (17)). The preconsolidation relative density (γ_0) was determined from the ordinate intercept of the logarithmic pressure–density relationship. A detailed discussion and summary of the compressibility parameters determined using these different techniques is described in Section 4.2.2.

3.4. Roller compaction

The development formulation described in Section 3.1 was roller compacted using an Alexanderwerk WP 120 × 40 V roller compactor. The equipment can be fitted with either 25 mm or 40 mm width rolls, each having a 120 mm diameter. This roller compactor has an instrumented control system to ensure set points are attained. The key controls are roll pressure, roll separation (gap), roll speed and screw feeder speed. The roll pressure is specified as the hydraulic pressure in bar. A roll force calibration coefficient is provided of 0.369 kN/bar for both roll width configuration. The equipment operates in either gap controlled or screw speed controlled configuration. With the former, the roll pressure, roll separation and roll speed set points are specified and the equipment moderates the screw feeder speed to achieve the desired roll separation. In the latter configuration, the roll pressure, roll speed and screw feeder speed are specified and the roll separation varies subject to the other set points. For the experiments described in this paper, both configurations were utilized. Ribbons were manufactured for a range of operating parameters using both the 25 mm and the 40 mm roll width assemblies. Ribbon fragments were sampled immediately following the initial ribbon breaker. Subsequently, the ribbon fragments are milled in the granulator assembly equipped along with the roller compactor to produce granules. However, analysis of the granules (and subsequent tablets) is beyond the scope of this paper. A combination of knurled and smooth rolls was used to reduce material sticking.

3.5. Ribbon relative density (RD) measurements

Ribbon samples collected from the roller compaction operation were analyzed for relative density values. The ribbon relative density, as given by Eq. (10), requires both true density and envelope density measurements. The ribbon true density measurements were determined by using a helium pycnometer (Accupyc 1330, Micromeritics Instrument Corp., Norcross, GA, USA) following the manufacturer recommended procedures. The envelope density of the ribbon was determined using Geopyc envelope density analyzer (Geopyc 1360, Micromeritics Instrument Corp., Norcross, GA, USA). More details about the ribbon relative density measurement methodology can be found elsewhere (Zinchuk et al., 2004).

4. Results and discussion

4.1. Small-scale roller compaction experiments

As part of the preliminary study to establish an initial operating range of the roller compactor, small-scale roller compaction experiments (batch size of approximately 600 g) were conducted

Table 1
Small-scale roller compaction experimental design.

Batch	Intra-granular lubricant level (%)	Roll pressure (bar)	Screw speed (rpm)	Roll speed (rpm)
1	0.25	20	35	5
2	0.75	20	35	10
3	0.25	60	35	10
4	0.75	60	35	5
5	0.25	20	75	10
6	0.75	20	75	5
7	0.25	60	75	5
8	0.75	60	75	10
9	0.5	40	55	7.5
10	0.5	40	55	7.5
11	0.5	40	55	7.5

using a 25 mm width roller assembly. A wide range of roller compaction process parameters was explored as illustrated in Table 1. A fractional factorial design (2^{4-1}) was implemented with the following four key factors: roll pressure, roll speed, screw speed and intra-granular lubricant amount (magnesium stearate). The experiments were carried out in run order (randomized) to eliminate any bias introduced by running in a structured non-random way (standard order). Experiments 9–11 (standard order) represent the centre points of the operating window.

Following experience and other authors, ribbon relative density is used as an indicator of roller compacted product quality. For each experimental batch ribbon samples were collected during steady state operation and the ribbon relative density was determined using the method described in Section 3.5. Table 2 shows the experimental design responses in terms of relative ribbon density, ribbon porosity measurements and mass throughput. The measured ribbon density showed a wide range from 0.689 to 0.821. Statistical analysis indicated that the ribbon density values were not significantly influenced by the level of intra-granular lubricant used in this study. Additionally, the mass throughput covered a wide range from 5.4 to 13.1 kg/h, representing an almost 2.5-fold increase in throughput. The mass throughput was also found to be a strong function of screw speed, which is consistent with Eq. (14). As an aside, the mass balance described in Eq. (12) and Eq. (13) can be used to estimate the ribbon relative density based on measurement of the mass throughput. In this case the discrepancy between the estimated and measured ribbon relative densities for all 11 batches was less than 1%.

4.2. Estimation of model parameters from roller compaction experiments

4.2.1. Estimation of screw speed constant

The experimental design runs, as described in Section 4.1, were performed using a screw speed control configuration and the roll separation was left as a floating variable. However, the roll separation was also monitored and recorded during the steady state operation for each run. The roll separation was found to be in the range 1–3.5 mm, depending upon the processing conditions. The screw constant (c_S) was estimated using Eq. (15), as described in Section 2.3.1. Fig. 5 shows the experimental data from the experimental design plotted using this approach. The data points lie on a straight line passing through the origin, as predicted by the equation. There is perhaps some small evidence of deviation at high screw speed to roll speed ratios, which may be due to material slippage as the screw approaches high rotation rates. The gradient, which corresponds to the screw constant, was obtained from a linear regression fit to this data. Here, the screw constant is 2.6 g, which corresponds to the mass of powder delivered for a full rotation of the screw. Interestingly, although intra-granular lubricant level was varied within the experimental design, it had no significant influence on the throughput.

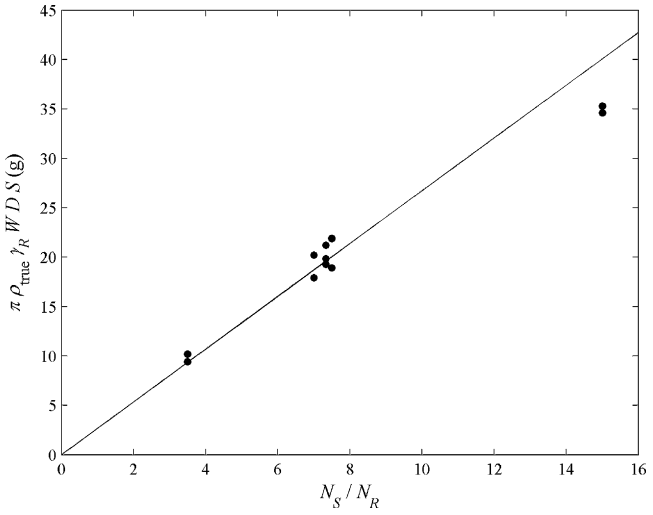

Fig. 5. Roll compactor data plotted using Eq. (15). Data fitted with $R^2 = 0.92$. The gradient, which corresponds to the screw constant, is 2.6 g.

Table 2
Experimental design responses.

Batch #	Ribbon relative density (γ_R)	Ribbon porosity (%)	Mass throughput (kg/h)
1	0.705	29.49	5.4
2	0.720	27.96	5.7
3	0.781	21.88	6.1
4	0.821	17.90	6.1
5	0.696	30.38	11.3
6	0.689	31.06	10.6
7	0.801	19.90	10.4
8	0.815	18.49	13.1
9	0.759	24.11	8.7
10	0.769	23.11	9.5
11	0.793	20.73	8.9

4.2.2. Estimation of compaction parameters (K and γ_0)

Using the experimental design process parameters (Table 1) and associated responses (Table 2) the compaction parameters were estimated using Eqs. (16) and (17), as described in Section 2.3. For comparison, the compaction parameters were also estimated using uniaxial compression test as described in Section 3.3. Compaction parameters estimated from both these methods are summarized in Table 3.

There are some differences between the uniaxial test measured properties and the inferred properties from the roller compaction data. Primarily, compression within the roller compactor is not entirely confined as compared to its state in the uniaxial compression test. Additionally, measurement of the ribbon density after roller compaction represents an 'out of die' measurement, in comparison to the 'in die' measurement acquired from uniaxial compression. After leaving the roller compactor, it is expected that there will be some degree of elastic recovery of the ribbon, prior

Table 3
Estimated compaction parameters from uniaxial compression technique and from roller compaction (RC) experimental data.

Compaction parameter	Uniaxial measurement	RC experimental measurement
Compressibility factor (K)	6.75	7.57
Preconsolidation relative density (γ_0)	0.44	0.38

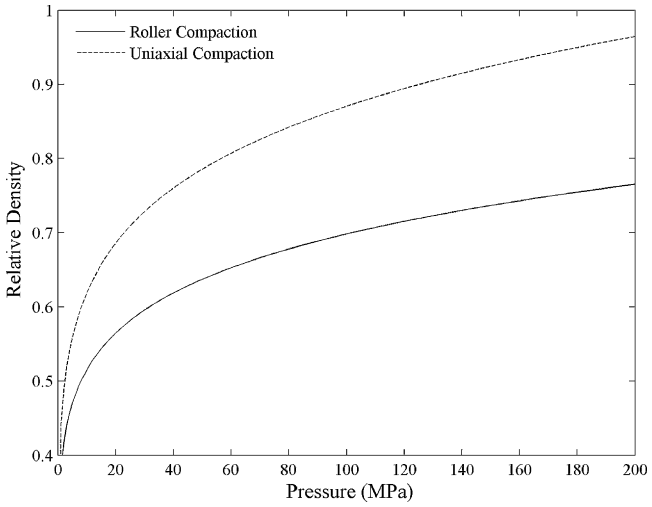

Fig. 6. Comparison of pressure density relationship inferred from ribbon density measurement and measured using uniaxial compression.

to measurement of its density. This recovery would be expected to reduce the apparent densification of the material for a given applied pressure.

All these factors suggest that using the uniaxial compaction data directly will typically lead to an over-prediction of ribbon density. Fig. 6 compares the pressure–density relationships summarized in Table 3. From this figure, the over-prediction is clear. Therefore the material parameters estimated from the roller compaction experiments were used for any modeling predictions discussed in the remainder of this paper. It is worth commenting that if the source roller compaction data contain an insufficient range of ribbon densities, satisfactory predictions can still be made by using the uniaxial compression test compressibility directly, and purely fitting the preconsolidation ribbon density with the roller compaction data. This approach essentially compensates for the differences between the static and the dynamic approaches by incorporating the differences into this single parameter.

4.3. Using the model to predict the influence of process parameter changes on ribbon density

Following the main experimental design (Table 1), several batches were manufactured to confirm the level of prediction capable from the model, using the estimated material parameters. Table 4 summarizes the input set points and measured ribbon density for these batches. In all cases, there is an excellent level of prediction of the ribbon density, with a RMSE (root mean square error) of 0.9% for the three batches.

4.4. Using model to predict process parameters required to achieve target ribbon density

With the model exhibiting excellent predictive capabilities for the influence of process parameters on ribbon density, the model was used to predict suitable process parameters in order to achieve a target ribbon density when changing from a screw controlled to a roll separation controlled configuration, but still using the same roll width of 25 mm. An intermediate ribbon relative density target of 0.754 was selected as an objective. In Section 2.4 it is demonstrated that to achieve a specific ribbon density, there exists a range of potential process parameters. It is only by posing further constraints (for example output throughput, or roll separation) that a unique combination of process parameters can be determined. For this investigation, three batches were run with three different target roll separations from 1.4 to 2.4 mm. Using Eq. (11), a suitable roll pressure was calculated for each batch. The predicted roll pressures are shown in Table 5.

Table 5
Predicted process parameter (roll pressure) to achieve target ribbon relative density.

Batch	Target ribbon relative density	Roll separation (mm)	Predicted roll pressure (bar)
15	0.754	1.8	32.8
16	0.754	2.4	37.9
17	0.754	1.4	28.9

Due to the interaction between roll separation and roll pressure (roll separation force) on the ribbon relative density, it is apparent from these predictions that an increase in roll separation will require an increase in roll pressure in order to achieve the same peak pressure (and hence ribbon density).

Due to the equipment capability, the roll pressures were rounded to the nearest whole number and the experiments performed, with the results presented in Table 6. Overall, the batches produced ribbon density close to the target range, indicating that the model provided adequate prediction of process parameters. The RMSE between the measured and predicted ribbon densities was calculated to be 1.3%.

4.5. Using model to predict influence of geometry and scale changes on ribbon density

The Alexanderwerk WP120 roller compactor can be configured using a 25 mm or a 40 mm width set of rollers. Early in development, it is advantageous to use the 25 mm width rollers to produce small size batches. However, as the process is scaled-up and transferred to a manufacturing environment, it will typically move to the larger 40 mm width rollers or a larger roller compactor. The roller compaction modeling approach as illustrated in this paper can accommodate the change in equipment geometry and calculate the required change in process parameters in order to achieve a consistent ribbon density. Results from the scale-up experiments are shown in Table 7. The predicted roll pressures are shown in order to achieve the target ribbon densities, for an experimental design varying both roll separation and ribbon density. The roll pressures were calculated using the material parameters determined from the small-scale (25 mm roll width) experiments and changing the geometric parameters in Eq. (11). The level of prediction for the ribbon density is excellent, with an overall RMSE of 1.0% between the predicted and measured values, demonstrating a ‘right first time’ approach to scale-up of the roller compaction process.

Table 4
Confirmatory batches to test level of prediction from model.

Batch	Roll pressure (bar)	Screw speed (rpm)	Roll speed (rpm)	Roll separation (mm)	Measured ribbon relative density	Predicted ribbon relative density	% Error
12	42	55	7.5	Variable	0.779	0.779	0.31
13	34	55	7.5	Variable	0.762	0.756	0.47
14	34	50	7.5	Variable	0.749	0.761	1.95

Table 6
Experimental data from batches designed to achieve a target ribbon density for varying roll separation.

Batch	Roll pressure (bar)	Screw speed (rpm)	Roll speed (rpm)	Roll gap (mm)	Predicted ribbon relative density	Measured ribbon relative density	% Error
15	33	Variable	7.5	1.8	0.754	0.731	3.19
16	38	Variable	7.5	2.4	0.754	0.740	1.88
17	29	Variable	7.5	1.4	0.754	0.755	0.11

Table 7
Results from scale-up study (using 40 mm width rollers), showing excellent agreement between the target and measured ribbon densities.

Batch	Batch size (kg)	Roll pressure (bar)	Roll speed (rpm)	Roll separation (mm)	Target ribbon density	Measured ribbon relative density	% Error
18	2.5	50	8.5	1.6	0.75	0.740	2.01
19	2.5	63	8.5	1.6	0.78	0.778	0.04
20	2.5	61	8.5	2.4	0.75	0.753	0.17
21	2.5	77	8.5	2.4	0.78	0.772	0.75
22	10	63	8.5	2.0	0.77	0.751	2.10

4.6. Overall discussion

In this paper, a practical application of roller compaction process modeling has been presented, demonstrating the utility of the approach with respect to excellent prediction of the key intermediate of ribbon density as a function of process parameters and excellent prediction of appropriate process parameters to achieve target ribbon densities for two separate geometrical configurations. Pragmatically the model can be calibrated using existing process data to estimate the underlying material parameters. The model allows the roller compaction process to be considered independent of scale (equipment geometrical parameters), by calculating the peak pressure experienced by the material between the rollers as a function of both process and geometric parameters. To demonstrate this, all the experimental data presented so far are plotted in Fig. 7. The peak pressure, P_{max} takes account of the various process and geometric parameters, such that the underlying pressure/density relationship of the formulation is revealed and shown to be consistent across the different experimental configurations.

This provides a clear route for changing process parameters to achieve target outputs (for example throughput, without changing ribbon density), and also transferring a process between equipment (and site), without impacting on the product quality. This approach also provides a clear justification for process parameter and equipment flexibility in the context of a pharmaceutical design space based on a proven acceptable range of peak pressures, or achieving target intermediate quality attributes, such as ribbon density.

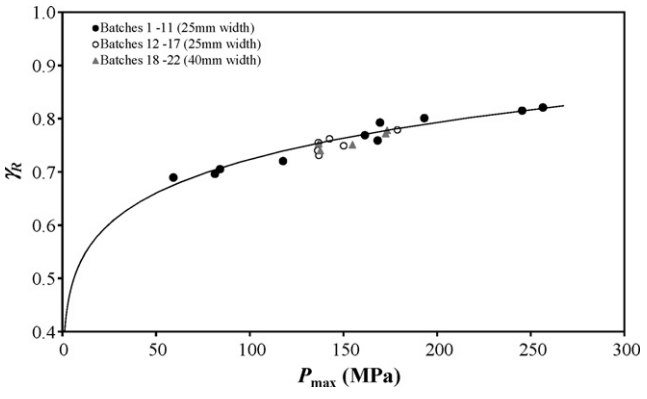

Fig. 7. Summary of all roller compaction experimental data for two different roller width configurations, compared with the roller compaction model (continuous line).

5. Conclusions

A method was presented to estimate material properties from roller compaction data generated using roll separation or screw controlled configurations. These estimated material properties can be more directly useful for prediction of ribbon density, as they include the differences in predensification of the material and post-compression recovery. The model was found to provide excellent prediction of the influence of process parameters on ribbon density. In addition, the model accurately determined appropriate process parameters to achieve target output ribbon densities for two different geometrical configurations (scales). Additionally the peak pressure predicted by the model was demonstrated to be a useful scale-independent parameter, allowing the underlying formulation compaction behavior to be presented for a range of roller compaction process parameters and geometric configurations.

Acknowledgments

The authors would like to thank Jessica Miller, Peter Brush and Mark McLaughlin for their work in producing the roller compaction manufacturing data used in this paper and also for valuable discussions.

References

Adeyeye, M. C. (2000). Roller compaction and milling pharmaceutical unit processes: Part I. *American Pharmaceutical Review*, *3*, 37–42.

Bindhumadhavan, G., Seville, J. P. K., Adams, M. J., Greenwood, R. W., & Fitzpatrick, S. (2005). Roll compaction of a pharmaceutical excipient — Experimental validation of rolling theory of granular solid. *Chemical Engineering Science*, *60*(14), 3891–3897.

Davies, N. P., & Newton, M. J. (1996). Mechanical strength. In G. Alderborn, & C. Nystrom (Eds.), *Pharmaceutical powder compaction technology* (pp. 165–192). New York: Marcel Dekker.

Dec, R. T. (1991). Study of compaction process in roll press. *Proceedings of the Institute for Briquetting and Agglomeration*, *22*, 207–218.

Dec, R. T., Zavaliangos, A., & Cunningham, J. C. (2003). Comparison of various modeling methods for analysis of powder compaction in roller press. *Powder Technology*, *130*, 265–271.

Gereg, G. W., & Cappola, M. L. (2002). Roller compaction feasibility for new drug candidates — Laboratory to production scale. *Pharmaceutical Technology*, *26*, 14–23.

Guigon, P., Simon, O., Saleh, K., Bindhumadhavan, G., & Seville, J. P. K. (2006). Chapter on roll pressing. In *Granulation and coating of fine powders (Handbook of Powder Technology S.)*. Amsterdam: Elsevier Publication.

Hancock, B. C., Colvin, J. T., Mullarney, M. P., & Zinchuk, A. V. (2003). The relative density of pharmaceutical powders, blends, dry granulations and immediate release tablets. *Pharmaceutical Technology*, (April), 64–80.

Jenike, A. W., & Shield, R. T. (1959). On the plastic flow of coulomb solids beyond original failure. *Journal of Applied Mechanics Transaction ASME 81, Series E*, *26*, 599–602.

Johanson, J. R. (1965). A rolling theory for granular solids. *ASME, Journal of Applied Mechanics Series, E*, *32*(4), 842–848.

Katashinskii, V. P. (1986). Analytical determination of specific pressure during the rolling of metal powders. *Soviet Powder Metallurgy and Metal Ceramics*, *10*, 765–772 [in Russian].

Loginov, Y., Bourkine, S. P., & Babailov, N. A. (2001). Cinematics and volume deformations during roll-press briquetting. *Journal of Materials Processing Technology*, *118*, 151–157.

Miller, R. (1997). Roller compaction technology. In D. M. Parikh (Ed.), *Handbook of pharmaceutical granulation technology* (pp. 99–150). New York: Marcel Dekker.

Peschl, I. A. S. Z., & Colijn, H. (1977). New rotational shear testing technique. *Journal of Powder & Bulk Solids Technology*, *1*, 55–60.

Pietsch, W. (1991). *Size enlargement by agglomeration*. New York: John Wiley & Sons Ltd.

Rowe, R. C., & Roberts, R. J. (1996). Mechanical properties. In G. Alderborn, & C. Nystrom (Eds.), *Pharmaceutical powder compaction technology* (pp. 283–322). New York: Marcel Dekker.

Schulze, D. (1996). Flowability of bulk solids—Definition and measuring techniques, Part I and II. *Powder and Bulk Engineering* 10, 4, pp. 45–61, 10 (1996) 6, pp. 17–28.

Seville, J. P. K., Perera, L. N., Greenwood, R. W., & Bentham, C. (2001). Roll granulation: principles and applications. In A. F. B. Van der poel, A. F. B. Van der poel, et al. (Eds.), *Advances in nutritional technology 2001* (pp. 71–82). Netherlands: Wageningen Press.

Zinchuk, A. V., Mullarney, M. P., & Hancock, B. C. (2004). Simulation of roller compaction using a laboratory scale compaction simulator. *International Journal of Pharmaceutics*, *269*, 403–415.